A01-34334

AIAA 2001-3645

Plasma Propulsion for Three Terrestrial Planet Finder Architectures: Free-Flying, Monolithic and Tethered

Kurt A. Polzin and Edgar Y. Choueiri
Electric Propulsion and Plasma Dynamics Laboratory
Applied Physics Group

Pinchas Gurfil and N. Jeremy Kasdin
Dynamics and Controls Group

Mechanical and Aerospace Engineering Department
Princeton University, Princeton, NJ 08544
USA

37th AIAA/ASME/SAE/ASEE
Joint Propulsion Conference and Exhibit
8-11 July 2001 / Salt Lake City, UT

Plasma Propulsion for Three Terrestrial Planet Finder Architectures: Free-Flying, Monolithic and Tethered

K.A. Polzin[*], **E.Y. Choueiri**[†], **P. Gurfil**[‡] and **N.J. Kasdin**[§]
Mechanical and Aerospace Engineering Department
Princeton University, Princeton, NJ 08544

AIAA 2001-3645 [¶]

July 10, 2001

Abstract

A systems-level trade-off study is presented comparing the propulsion requirements and associated final masses for different architectural implementations of the Terrestrial Planet Finder (TPF) mission. The study focuses on the mN-level propulsion chores associated with rotation and repointing. Three interferometer configurations; free-flying, monolithic and tethered; lead to estimates of power requirements and spacecraft masses associated with different plasma propulsion systems required to maneuver the interferometer throughout its lifetime. The parametric study includes the following plasma propulsion options: Hall thruster, Field Emission Electric Propulsion (FEEP), Ablative Pulsed Plasma Thruster (APPT), Ablative Z-pinch Pulsed Plasma Thruster (AZPPT) and Gas-Fed Pulsed Plasma Thruster (GF-PPT). For the different thruster and architecture combinations, it is found that the initial mass for a system falls between 3200 and 4200 kg. Also, in general, for a given architecture, the tether has the lowest initial mass followed by the free flyer and the monolith. Finally, the initial mass was found not to be particularly sensitive to the type of plasma propulsion system so the choice should be made based on technological readiness, systems integration considerations and spacecraft contamination issues associated with the chosen system.

Nomenclature

a - square side length [m]
g_0 - gravitational acceleration [m/s^2]
I - moment of inertia [kg-m^2]
$I_{bit\ max}$ - max. deliverable impulse bit [mN-s]
$I_{s/c}$ - per spacecraft I [kg-m^2]
I_{sp} - specific impulse [s]
M - moment applied to spacecraft [N-m]
$M_{s/c}$ - per spacecraft M [N-m]
$m_{s/c}$ - per spacecraft m_i [N-m]
m_{comb} - combiner mass [kg]
m_f - final (propellantless) mass [kg]
m_{fixed} - fixed mass excluding propulsion [kg]
m_i - initial (total) mass [kg]
$m_{p\,(fixed)}$ - fixed power supply mass [kg]

[*]Graduate Student, Electric Propulsion & Plasma Dynamics Lab (EPPDyL). Applied Physics Group. Member AIAA.
[†]Chief Scientist at EPPDyL. Assistant Professor, Applied Physics Group. Senior Member AIAA.
[‡]Post-Doctoral Researcher, Dynamics and Controls Group. Member AIAA.
[§]Assistant Professor, Dynamics and Controls Group. Senior Member AIAA.
[¶]Presented at the 37th AIAA Joint Propulsion Conference, Salt Lake City, Utah, July 8-11, 2001. Copyright © by authors. Published by the AIAA with permission.

m_{pay} - payload mass [kg]
m_{ppu} - power processing unit (PPU) mass [kg]
m_{prop} - propellant mass [kg]
m_{ps} - total power supply mass [kg]
$m_{ps\,(thr)}$ - thruster power supply mass [kg]
m_{tank} - tankage mass [kg]
$m_{thr\,(fixed)}$ - fixed thruster mass [kg]
P_{fixed} - constant (fixed) power required [W]
P_{max} - maximum required power [W]
P_{min} - minimum required power [W]
P_{thr} - required power for thruster [W]
P_{total} - total required power [W]
R - circular radius [m]
$R_{s/c}$ - per spacecraft R [m]
T/P - thrust-to-power ratio [mN/W]
T_{max} - maximum deliverable thrust [mN]
t_{mis} - mission length [s]
T_{req} - required thrust [mN]
t_{rot} - rotational period [s]
$T_{s/c}$ - per spacecraft T_{req} [mN]
x,y - lateral spacecraft dimensions [m]
α - specific mass [kg/kW]
α_a - average angular acceleration [rad/s^2]
Δt - time for a maneuver [s]
ΔV - characteristic mission velocity [m/s]
$\Delta\theta$ - repointing angle [rad]
η - thruster efficiency
ω - rotational velocity [rad/s]

1 Introduction

The motivation behind this work is NASA's Terrestrial Planet Finder (TPF) mission described in the science working group book [1]. This is a cornerstone project in NASA's Origins program to look for planets capable of supporting life outside the solar system. One imaging approach being considered is the use of a nulling interferometer to block the starlight, thus allowing the companion planet to be more easily seen.

One implementation being considered would have TPF performing several different missions over its lifetime including planet finding, medium depth spectroscopy, deep spectroscopy and astrophysics ([1], pgs. 87-89). The planet finding and spectroscopy missions currently under consideration involve using multiple, free-flying telescopes following a closed path with baselines between 75 and 135 meters to form a sparse aperture interferometer. In this configuration, planet finding, where TPF simply observes a star system to look for planets which are candidates for further investigation, is currently scheduled to occupy 1.4 of the 5 years of TPF's design lifetime using a per-star system observation time of 8 hours. Medium depth spectroscopy is scheduled to take 1.4 years, assuming an observation period of 3 days, while deep spectroscopy is scheduled for 0.7 years with an observational period of 2 weeks ([1], pgs. 87-88). Astrophysical observations require the baseline to be changed from 75 to 1000 meters. This has been projected to take 1.5 days per observation and occupy 1.3 years of the total mission time ([1], pgs. 88-89).

In this paper we examine only the primary mission objective, that of planet finding. Three possible configurations for the interferometer are considered:

1. a free-flying formation of spacecraft,
2. a monolithic assembly over a deployable truss,
3. a tethered constellation.

In all three cases, we assume that there are four collectors and a single combiner used as a sparse aperture, rotating interferometer. It should be noted that the monolith and tethered configurations, both considered as structurally connected, may not be able to perform some of the other tasks considered due to their more constrained baseline.

A previous study by Stephenson [2] looked at trade-offs in metrics of initial mass, mission adaptability and mission capability for two interferometer configurations, free-flying and monolithic. That study did not, however, take into account the mass of the power supply required to operate a plasma propulsion system, which could become substantial for some options. It also did not explore changes to the metrics which might arise from choosing a plasma propulsion option with different characteristic performance values.

We focus here on the trade-offs between the propellant mass savings and the power mass penalties associated with the use of plasma propulsion with three interferometer configurations. Also, for each configuration different plasma propulsion systems representing a wide range of available performance characteristics are considered.

The ΔV for each architecture is only for mN-level propulsion tasks performed during planet finding and not μN-level tasks that might be needed for fine positioning of an interferometer. The ΔV is calculated relative to a reference point in space, located at the rotational center of the interferometer, which itself has some orbital trajectory. The ΔV required for the system to reach this orbital trajectory is not included in this study. From a propulsion point of view, planet-finding is the 'worst-case' scenario in that more propellant, thrust and power are needed for this mission. For the purposes of this study, we will assume this 'worst-case' mission to occupy the entire 5 year lifetime of TPF. The propulsion systems considered are:

1. Hall Thrusters,
2. Field Emission Electric Propulsion (FEEP),
3. Ablative Pulsed Plasma Thrusters (APPT),
4. Ablative Z-pinch Pulsed Plasma Thrusters (AZPPT),
5. Gas-Fed Pulsed Plasma Thrusters (GF-PPT).

A recent description of each of these systems can be found in ref. [3].

Section 2 discusses how the spacecraft power requirements and mass are broken down and contains reference data on the performance of all the thrusters considered in this study. In section 3, the mission involving the free-flying interferometer is explored. Here, two different free-flying scenarios will be described and the mass, power and ΔV trade-offs for each propulsion system in this architecture will be discussed. Next, the trade-offs associated with the use of a monolithic interferometer configuration to complete a comparable reference mission are studied. A tethered interferometer is then studied as a third alternative, and the effects of using different propulsion systems on this configuration are explored. Finally, a head-to-head comparison of each of the propulsion system/configuration combinations is made highlighting the strengths and weaknesses of each.

2 Power, Mass and Propulsion

2.1 Power Determination

The power requirements can be split into two basic parts, where the total power required is just the sum of the power needed to (a) operate the spacecraft instruments and perform housekeeping tasks and (b) P_{thr}. Under the assumption that power needs for task (a) are constant, the power requirements scale with P_{thr}. We find this P_{thr} by taking the maximum required thrust during the mission and dividing it by a given thruster's characteristic thrust-to-power ratio, T/P.

2.2 Mass Determination

Referencing Figure 1, the initial (total) spacecraft mass is made up of a final mass and a propellant mass. The propellant mass is itself also a function of final mass through the rocket equation. The final spacecraft mass can be divided into three general parts: m_{pay}; mass of equipment to generate a constant power for the spacecraft instruments and housekeeping tasks, $m_{p\ (fixed)}$; and mass contributions derived from the propulsion system. Breaking down the thruster contribution even further, m_{tank} is associated with propellant storage and feeding, $m_{thr\ (fixed)}$ is the mass of the thruster and its associated hardware times the number of thrusters employed, and a power-dependent thruster mass is associated with the generation of P_{thr}. The tankage mass is taken at 10% of the propellant mass in gas-fed devices and 5% in solid-propellant (ablative) devices throughout this paper. Finally, one can divide the power-dependent thruster mass into two terms. The first is the mass of the power supply, m_{ps}, which contains all the hardware necessary to generate the power for the thruster to operate. The second, m_{ppu}, is the mass of the equipment needed

to take the power provided by the spacecraft bus and step it up to the correct voltage and current requirements for the given thruster. Typically, this is handled by multiplying the power required by a given power processing unit specific mass, α, which is a technology-dependent characteristic parameter for any given thruster.

Solar panels are sized using a spreadsheet giving the array voltage, current and power output.[4] First, the number of solar cells in a string are selected so the maximum power is provided to the spacecraft at a voltage of about 36 Volts. Then the number of parallel strings are selected so that the power output of the array is equal to the total power required by the spacecraft. This gives a solar array size and mass.

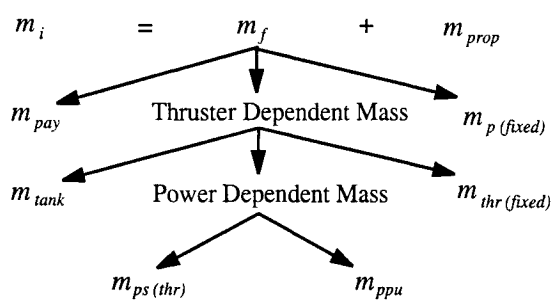

Figure 1: Typical mass breakdown for a plasma propulsion system.

The initial mass of the spacecraft determines the thrust and power requirements for the thruster and the power supply mass is readjusted to provide the needed power. An iterative methodology is used to converge to the correct initial spacecraft mass and required power. All cases are assumed to have at least one Li-ion battery at a mass of 11.9 kg. In some cases, additional batteries are added to reduce the size of solar arrays, which are here kept under 40 kg. This can only be done in cases where there is a long enough delay between thruster firings to allow the battery bank to charge up again.

2.3 Propulsion Systems

Table 1 contains a list of the relevant operating parameters for each plasma thruster studied in this paper. These numbers are used to perform the mission analysis throughout the paper. The thrusters are the Hall thruster, Field Emission Electric Propulsion (FEEP), Ablative Pulsed Plasma Thruster (APPT), Ablative Z-pinch Pulsed Plasma Thruster (AZPPT) and Gas-Fed Pulsed Plasma Thruster (GF-PPT). Descriptions and background on each of these devices can be found in refs. [3]-[9]. The fixed mass per thruster for all of these systems are assumed to be about 5 kg, except FEEP which is assumed to be 3 kg. It turns out, however, in all cases that this fixed mass is negligible compared to the mass of the spacecraft and propellant.

	Hall	**FEEP**	**APPT**	**AZPPT**	**GF-PPT**
Fuel	(Xe, Kr)	(Cs)	(Teflon)	(Teflon)	(Xe, Ar)
I_{sp}	1600 s	10000 s	1500 s	400 s	7000 s
$I_{bit\ max}$	-	-	2.5 mN-s	3.4 mN-s	40 μN-s
T_{max}	80 mN	5 mN	-	-	-
T/P ratio	60 μN/W	16 μN/W	30 μN/W	45 μN/W	7 μN/W
η	50%	80-100%	2-15%	2-8%	2-13%
α	4 kg/kW	10 kg/kW	4 kg/kW	4 kg/kW	4 kg/kW
References	[3, 5]	[5, 6]	[5, 7]	[8]	[9]

Table 1: Summary of characteristics for different plasma propulsion systems.

	Outer Collector	Inner Collector	Combiner
m_{fixed}	644 kg	643 kg	605 kg
P_{fixed}	325 W	325 W	866 W

Table 2: Free flyer fixed mass and power levels excluding those associated with propulsion. After ref. [1], pg. 111.

3 Free-Flying Interferometer

The first mission examined will be that consisting of several free-flying spacecraft moving in formation to form a sparse-aperture array. The fixed masses associated with each spacecraft and the power requirements excluding those for the propulsion system are taken from ref. [1], pg. 111. There are five spacecraft: two outer collectors, two inner collectors and a combiner. The masses and power requirements are given in Table 2.

Different types of closed path revolutions have been previously studied by Stephenson [2]. In that work, two different scenarios for the free flyer are developed.

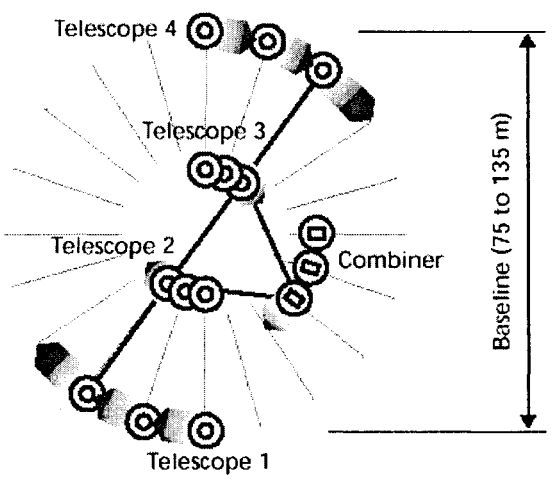

Figure 2: Flight path during planet finding for a free-flying interferometer following a circular path. (from [1], pg. 108). A 135m baseline is assumed for this study.

In the first scenario, illustrated in Figure 2, the outer and inner collectors and the combiner revolve in a circle around some fixed point relative to the system with the collectors remaining in a straight line for the entire revolution. While on this flight path, the spacecraft must fire their thrusters continuously at a low thrust level to keep them on the circular paths.

The total ΔV needed to complete one closed, circular path is given by [2]

$$\Delta V_c = 4\pi^2 R/t_{rot}. \tag{1}$$

The total ΔV for the mission is given by

$$\Delta V_{c\ total} = 4\pi^2 R\, t_{mis}/t_{rot}^2, \tag{2}$$

where t_{mis} is taken in this study as 5 years. The mass of each spacecraft is given by the rocket equation as

$$m_i = m_f e^{\Delta V_{c\ total}/(I_{sp}\, g_0)}, \tag{3}$$

with the mass of the propellant being the difference between m_i and m_f. The required thrust is

$$T_{req} = m_i \omega^2 R = m_i \left(\frac{2\pi}{t_{rot}}\right)^2 R. \tag{4}$$

Finally, the power needed for propulsion and the mass of the power processing unit are

$$P_{thr} = T_{req}/\left(T/P\right), \qquad m_{ppu} = \alpha P_{thr}. \tag{5}$$

The second scenario developed by Stephenson [2] was that of a closed flight path consisting of a square instead of a circle. In this scenario, the spacecraft follow a square path equal in perimeter to the circular path. The spacecraft thrusters have to fire at the corners of the square path with a thrust level that is higher than that of the circular path.

For a square path with perimeter and rotational period that are equal to those of a circular path of radius R, the ΔV required for one rotational period is [2]

$$\begin{aligned} \Delta V_s &= 0.573\left(4\pi^2 a\right)/t_{rot} \\ &= 0.573 \Delta V_c\, a/R. \end{aligned} \tag{6}$$

(a for a 135 meter baseline is 106 meters.) The total ΔV for the mission lifetime is then

$$\begin{aligned} \Delta V_{s\ total} &= 0.573\left(4\pi^2 a\, t_{mis}\right)/t_{rot}^2 \\ &= 0.573\Delta V_c\, a\, t_{mis}/\left(t_{rot}\, R\right). \end{aligned} \tag{7}$$

The mass fraction is still given by equation (3). We assume that in order to change the spacecraft direction at the corners, the thrusters fire for 10% of the total rotational period. The necessary thrust in this case is given by the relation

$$T_{req} = m_i \Delta V_s/\left(0.1\, t_{rot}\right), \tag{8}$$

where the numerator is recognized as being the total impulse needed for the completion of one rotational period. Propulsive power requirements and PPU mass are still obtained from equation (5). The possible motivations using this path as opposed to the circular path are two-fold. One can achieve some reduction in the ΔV requirement for each spacecraft per revolution and the thrusters no longer need to be firing during the observation time, which serves to eliminate some potential noise in the data.

As mentioned earlier, we are only concerned in the present study with the mN-level thrusters needed to rotate the array about some reference point. Left out are the μN-level thrusters that will surely be needed to finely position the individual free flyers in the array so the tight tolerances required for interferometry can be maintained. This is not only an issue of additional mass due to a second set of thrusters, but also a technology readiness issue in that μN-level thrusters remain to be life-tested in space. Also, repointing of the array and attitude control have been neglected entirely since their associated ΔV is a fraction of that needed to constrain the rotational motion.

3.1 Representative Mission

For the free-flyer we make several assumptions about the spacecraft and mission. We assume planet finding is performed continuously for the entire mission lifetime. For the circular path, the thrusters fire for the entire rotational period, while they only fire over 10% of the rotational period for the square path when the spacecraft reaches a corner of the square. Finally, we assume an observation period of eight hours and a baseline of 135 meters. This baseline is relative to the circular flight path, with the square flight path conforming to the equal perimeter condition.

3.2 Results

In this section, the important calculated parameters for the free-flyer mission are presented for each spacecraft in the five-spacecraft array. There are results for both the circular and square flight paths using each of the five thrusters cited in Table 1. The parameters of interest are found in Table 3 for each spacecraft following the circular flight path and in table 4 for the square flight path. P_{total} represents the maximum power requirement of each spacecraft and assumes no subsystems are shut down while the thrusters are firing. P_{min} is the power level needed for the spacecraft without the thrusters firing, but does not include the power needed to charge any battery banks. (Note: the solar array has been sized to provide the power necessary to charge the batteries in between firings as well as to operate systems on the spacecraft. The batteries are assumed to discharge at 200 W each.) All spacecraft that follow a circular path and all but 2 that follow a square path have one battery. The exceptions are the outer collectors and combiner for the FEEP option (2 batteries), and for the GF-PPT option's inner collectors (2 batteries), combiner (4 batteries), and the outer collectors (14 batteries). As noted before, these extra batteries reduce the solar collector size by providing additional power during peak usage. Recall that FEEP and GF-PPTs require high power levels to produce thrusts comparable to Hall thrusters and APPTs due to their significantly lower T/P ratios. The outer collectors for the GF-PPT option give an extreme example of how low T/P ratios can impact the power supply mass.

	Hall	FEEP	APPT	AZPPT	GF-PPT
Outer Collector					
P_{thr} [W]	38	138	77	57	332
P_{total} [W]	363	463	402	382	647
m_{ps} [kg]	17.1	18.6	17.6	17.3	21.5
m_{ppu} [kg]	0.15	1.36	0.30	0.23	1.27
m_{prop} [kg]	24.9	3.9	25.4	100.1	5.7
m_i [kg]	716	686	717	792	702
Inner Collector					
P_{thr} [W]	12	46	25	17	106
P_{total} [W]	337	371	350	342	431
m_{ps} [kg]	16.7	17.3	16.9	16.8	18.1
m_{ppu} [kg]	0.05	0.45	0.10	0.07	0.42
m_{prop} [kg]	8.2	1.3	8.4	31.9	1.9
m_i [kg]	698	680	698	722	693
Combiner					
P_{thr} [W]	12	44	24	16	101
P_{total} [W]	878	910	890	882	967
m_{ps} [kg]	24.1	34.6	24.5	25.3	25.6
m_{ppu} [kg]	0.05	0.44	0.10	0.07	0.40
m_{prop} [kg]	7.8	1.2	8.0	30.4	1.8
m_i [kg]	667	659	668	690	663
Total m_i [kg]	3495	3391	3499	3716	3454

Table 3: Calculated parameters for free-flying spacecraft following a circular flight path and using different plasma propulsion systems. (For outer collectors: $m_{pay} = 644$[kg]; $\Delta V = 507$[m/s]. For inner collectors: $m_{pay} = 643$[kg]; $\Delta V = 169$[m/s]. For combiner: $m_{pay} = 605$[kg]; $\Delta V = 169$[m/s].) m_i includes tankage mass and fixed thruster mass assuming six thrusters per spacecraft.

3.3 Discussion

One notices immediately from comparing the circular and square paths that there is a slight ΔV advantage, and hence a slight propellant mass advantage, in using the square path. However, in all the cases that advantage is largely negated as the spacecraft must provide a large amount of power over a short time, and to do this requires more batteries, thus adding more weight, for power storage. For the circular path, the high I_{sp} of FEEP and GF-PPTs makes the overall spacecraft mass for these propulsion systems most attractive, while on the square path, it is their correspondingly low thrust-to-power ratio that makes these same thrusters unattractive. Also, current FEEP systems cannot produce the required thrust levels to complete the square path within the given assumptions. The AZPPT is plagued by low I_{sp} which translates to a high propellant mass. The Hall thruster and APPT have about the same masses for each path, meaning that they could be used if one wanted the spacecraft to have the versatility to travel either a circular or a square path. It is important to note that Hall thrusters operating at power levels below 500 W are currently not available but are in the research phase of development (c.f. [10, 11]).

	Hall	FEEP	APPT	AZPPT	GF-PPT
Outer Collector					
P_{thr} [W]	345	1294	697	505	3611
P_{min}/P_{max} [W]	325/670	325/1619	325/1022	325/831	325/3936
m_{ps} [kg]	18.9	37.7	23.1	20.6	181
m_{ppu} [kg]	1.40	12.80	2.75	2.00	12.8
m_{prop} [kg]	22.5	3.6	23.1	90.1	6.4
m_i [kg]	717	716	723	787	874
Inner Collector					
P_{thr} [W]	112	414	224	154	975
P_{min}/P_{max} [W]	325/437	325/739	325/549	325/479	325/1300
m_{ps} [kg]	16.8	20.1	16.8	16.8	30.0
m_{ppu} [kg]	0.44	4.20	0.88	0.61	4.20
m_{prop} [kg]	7.4	1.2	7.5	28.6	1.7
m_i [kg]	698	686	698	719	708
Combiner					
P_{thr} [W]	107	400	214	147	967
P_{min}/P_{max} [W]	866/973	866/1266	866/1080	866/1013	866/1833
m_{ps} [kg]	24.1	36.5	24.1	24.3	61.5
m_{ppu} [kg]	0.42	3.96	0.84	0.58	4.00
m_{prop} [kg]	7.1	1.1	7.2	27.4	1.7
m_i [kg]	667	664	667	687	702
Total m_i [kg]	3495	3470	3509	3699	3866

Table 4: Calculated parameters for free-flying spacecraft following a square flight path and using different plasma propulsion systems. (For outer collectors: $m_{pay} = 644$[kg]; $\Delta V = 456$[m/s]. For inner collectors: $m_{pay} = 643$[kg]; $\Delta V = 152$[m/s]. For combiner: $m_{pay} = 605$[kg]; $\Delta V = 152$[m/s].) m_i includes tankage mass and fixed thruster mass assuming six thrusters per spacecraft.

4 Monolithic Interferometer

While the free-flying spacecraft depend on the propulsion system to keep them all moving relative to one another, the monolith does not have that problem as all its components are physically connected by trusses. As such, once on station, the only propulsive requirements for the interferometer will be to spin it up to a given rotational speed for observation and to repoint it at different stars for observation. This repointing was totally neglected in the previous section on free-flying spacecraft.

The ΔV for the spin-up maneuver is given as

$$\Delta V_{spin} = \omega R = 2\pi R/t_{rot}, \tag{9}$$

where R has been taken to be the radius of the outer collectors for a conservative estimate. The moment needed to accomplish this maneuver is

$$M = I\alpha_a = I\frac{\omega}{\Delta t} = I\frac{2\pi/t_{rot}}{\Delta t}. \tag{10}$$

By assuming the components of the formation (collectors, connecting booms) are lumped masses, m_j, (lumped at their center of mass some distance, R_j, from the center of the monolith), and that the combiner has some finite dimension and a roughly uniform mass distribution, the moment of inertia becomes

$$I = \Sigma\, m_j R_j^2 + \frac{1}{12} m_{coll} \left(x^2 + y^2\right). \quad (11)$$

Assuming there are two thrusters firing symmetrically about the axis of rotation the thrust needed per thruster is

$$T_{req} = M/\left(2R\right). \quad (12)$$

For repointing maneuvers, the ΔV required is twice that given in eqn. (9) because one must accelerate and then slow down the spacecraft to turn it. The required ΔV is given as

$$\Delta V_{repoint} = 2\omega R = 2\frac{\Delta\theta}{\Delta t} R. \quad (13)$$

The necessary moment is now given as

$$M = I\alpha_a = I\frac{\Delta\theta}{2\Delta t^2}. \quad (14)$$

The total thrust is still given in eqn. (12). The total ΔV for the entire monolith mission can be written as

$$\Delta V_{total} = \Delta V_{spin} + \Delta V_{repoint}\left(t_{mis}/t_{rot}\right). \quad (15)$$

The spacecraft mass can be calculated from the rocket equation (3). As in the free flyer case, the total PPU mass and power required by the thruster are given by equation (5). The case with the most stringent power requirements (spin-up or repointing) should be the one analyzed to size the power supply system.

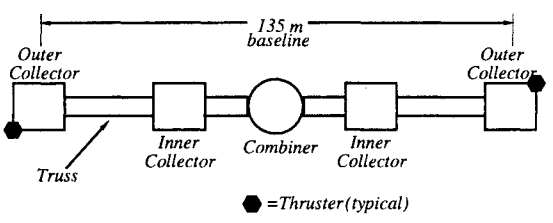

Figure 3: Configuration of the monolithic interferometer assumed for this study.

4.1 Representative Mission

It is important to make assumptions for this mission that are similar to those for the free-flyer so that the effects of the architecture change can readily be seen. As shown in Figure 3, there are still five separate optical components for the monolith; two outer collectors, two inner collectors and a combiner; except they are now connected by a rigid truss. The weight and power requirements of these components are assumed to be that of each similar component in the free-flyer scenario except now we take the mass and power needed for attitude control, communications and data management systems on each spacecraft and consolidate them to a central location in the combiner. The assumption is that while structurally connected, only one component for each of these tasks is needed and a weight and power requirement reduction can be realized by eliminating redundant components on the collectors. This serves to reduce the fixed mass and power requirements of the collectors given in Table 2 while maintaining the combiner fixed mass and power requirements at the same levels as in the free-flyer architecture. Also, one only needs thrusters and PPU systems on the outer collectors for spinning up and repointing the array while all the required power systems are to be located at the combiner, with power distributed through cables running throughout the truss to the collectors.

The outer truss sections in this study are taken at roughly 45 meters in length and are calculated, following Stephenson ([2], pgs. 45-46), to have a mass of 68 kg each while the inner ones are at half the length and the mass. The combined mass estimate for the truss and the deployment mechanism cited in Stephenson ([2], pg. 119) is 988 kg. We can subtract the truss section masses given above from this number to find the mass of the deployment mechanism. This deployment mass is assumed for this study to vary linearly with truss length and can be divided into three equal parts to be added into the masses of the combiner and the two inner collector modules. For moment of inertia calculations, the trusses and collectors are assumed to be lumped masses at a radius approximately equal to the distance from the monolith's center to the centroid of each component. The combiner is taken to be roughly a 3-by-3 meter box

with a uniform mass distribution.

The observation period is maintained as before at 8 hours with observations taking place over the entire 5-year mission of the interferometer. The monolith performs one spin-up maneuver at the beginning of its lifetime and then performs a repointing maneuver after each observation. The spin-up and repointing maneuvers are assumed to take 30 minutes to complete with a repointing angle of $\pi/8$ radians per maneuver. These numbers were chosen for this study in an attempt to keep the ΔV for the monolith nearly equal to the ΔV for the inner spacecraft of the free-flyer. For a repointing maneuver, the ΔV is very sensitive to the repointing angle and Δt. By increasing the angle or decreasing Δt by a factor of 2, the change in ΔV can easily translate into a doubling of the propellant mass. As can be seen in Fig. 3, there is an axis about which the moment of inertia is a minimum and two (by symmetry) about which it is a maximum. For a conservative ΔV estimate, the spinning and repointing are assumed to always be performed about the axis having the greater moment of inertia.

4.2 Results

Several calculated parameters are presented in Table 5. First, the payload masses of the collector and combiner modules are found in the caption and have been calculated under the assumptions stated in the previous subsection and using the data in Ref. [1], pg. 111. These masses reflect reductions due to the consolidation of certain subsystems. The power system and PPU masses are given separately to allow one the ability to compare the demands of this configuration with those of the free flyer in Tables 3 and 4. All the interferometer modules, fuel, power systems and trusses are included in m_i while P_{min}/P_{max} are the minimum and maximum power levels the system needs to provide. This assumes that while the thrusters are firing, no subsystems are shut down. All cases have at least one battery with the APPT possessing two, FEEP having three, and the GF-PPT having a bank of eight. These are the same Li-ion batteries as before.

4.3 Discussion

We see the monolith has a ΔV advantage with respect to the free flyer because the rigid truss eliminates the need to thrust during the revolution. Also, the sum of the power supply masses for a free-flying constellation (circular or square path) using a given propulsive option is in most cases larger than that of the monolith. The only exception is for the GF-PPT option following a circular path, and then the monolith's power supply mass is only marginally larger. Lastly, for the free flyer the optimum thrust vector of

	Hall	**FEEP**	**APPT**	**AZPPT**	**GF-PPT**
Outer Collector					
P_{thr} [W]	102	378	205	140	876
m_{prop} [kg]	6.6	1.0	6.7	25.6	1.5
m_{ppu} [kg]	0.41	3.80	0.82	0.56	3.50
Combiner					
m_{ps} [kg]	34.5	60.3	46.6	35.5	119.8
P_{min}/P_{max} [W]	1610/1815	1610/2366	1610/2020	1610/1890	1610/3362
Total m_i [kg]	4063	4065	4077	4103	4145

Table 5: Calculated parameters for a monolithic interferometer using different plasma propulsion systems. (ΔV = 152[m/s]. For outer collectors: m_{pay} = 593[kg]. For inner collectors: m_{pay} = 593[kg]. For combiner: m_{pay} = 605[kg].

the inner collectors passes through the outer collectors. In the monolith architecture, because the structure, and not the thrusters, constrain the rotational motion, no thrusters are required to fire "through" the outer collectors. It is expected that the contamination due to spacecraft/plume interactions will be decreased for the monolith architecture.

5 Tethered Interferometer

The assumptions of subsystem consolidation presented in the previous section are maintained for the case of a tethered interferometer with one major exception. Power and command signals can still be distributed to each spacecraft in the array through a tether, but the tether provides no real structural restraint from the point of view of performing maneuvers. It is desired that all five spacecraft remain in a straight line revolving about the combiner. However, each spacecraft has its own inertia to overcome and requires its own thruster system in this scenario so each can separately acquire the tangential velocity needed to maintain the system flight path. A small mass was added to the payload mass of the combiner (20 kg) and inner collectors (10 kg each) to account for the mechanism for extending/retracting the tether.

The ΔV for spinning up and spinning down a tethered system must now be calculated for each spacecraft individually since there is no longer a rigid structure between the modules. The per spacecraft ΔV for spinning up a spacecraft is

$$\Delta V_{spin} = \omega R_{s/c} = 2\pi R_{s/c}/t_{rot}. \tag{16}$$

An identical ΔV is incurred to slow a spacecraft down again. The moment that one must apply to each spacecraft for this maneuver is

$$M_{s/c} = I_{s/c}\alpha_a = I_{s/c}\frac{\omega}{\Delta t} = I_{s/c}\frac{2\pi/t_{rot}}{\Delta t}. \tag{17}$$

The moment of inertia for the collectors and combiner, respectively, are given for this maneuver as

$$\begin{aligned} \text{collector}: I_{s/c} &= m_{s/c}R_{s/c}^2, \\ \text{combiner}: I_{s/c} &= \tfrac{1}{12}m_{s/c}\left(x^2+y^2\right). \end{aligned} \tag{18}$$

As before, the ΔV needed per spacecraft repointing maneuver is

$$\Delta V_{repoint\ s/c} = 2\omega R_{s/c} = 2\frac{\Delta\theta}{\Delta t}R_{s/c} \tag{19}$$

and the needed moment per spacecraft is written as

$$M_{s/c} = I_{s/c}\alpha_a = I_{s/c}\frac{\Delta\theta}{2\Delta t^2}. \tag{20}$$

The moment of inertia can no longer be calculated by merely assuming the spacecraft to be lumped masses some distance from the axis of rotation because that distance is not very large relative to the spacecraft size. As such, for repointing all the spacecraft must now have their moment of inertia calculated as

$$I_{s/c} = \frac{1}{12}m_{s/c}\left(x^2+y^2\right) + R_{s/c}^2 m_{s/c}. \tag{21}$$

For both the spin-up/down and repointing maneuvers, the thrust and power requirements are

$$\begin{aligned} T_{s/c} &= M_{s/c}/R_{s/c}; \\ P_{s/c} &= T_{s/c}/\left(T/P\right); \\ m_{ppu} &= \alpha\, P_{s/c}, \end{aligned} \tag{22}$$

while the total ΔV is now

$$\Delta V_{total} = \left(\Delta V_{spin} + \Delta V_{repoint}\right)\left(t_{mis}/t_{rot}\right). \tag{23}$$

As before, the most severe case (spin-up/spin-down or repointing) should be used to size the spacecraft propulsion and power systems.

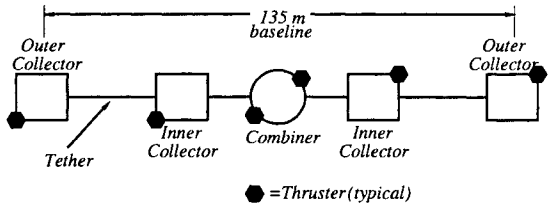

Figure 4: Configuration of the tethered interferometer assumed for this study.

5.1 Representative Mission

The assumptions here are similar to those for the monolith with one important exception. It is easier to repoint the system at a new target star when the tethers are retracted because the moment of inertia is lower. We assume that between observations, the spacecraft rotational velocities are slowed by thrusters and the tethers are retracted from the baseline of 135 meters down to a more compact size. The system then performs a repointing maneuver and again extends its components for another observation, accelerating back up to the observation rotational velocity. The spin-up and spin-down times are assumed to be 30 minutes each and the repointing maneuver is performed for 30 minutes over an angle of $\pi/8$ radians per maneuver, just as in the monolith case. Again, these values were chosen to keep the maximum ΔV of the tethered array roughly equal to the ΔV of the inner spacecraft in the free flyer architecture. Like the monolith, spin-up/spin-down and repointing maneuvers are always assumed to be performed about the axis with the greater moment of inertia. Unlike the monolith, the majority of the ΔV requirement for this configuration is due to the spin-up/spin-down maneuvers, while the repointing ΔV is small due to the reduced moment of inertia of the constellation with all tethers retracted.

	Hall	FEEP	APPT	AZPPT	GF-PPT
Outer Collector					
P_{thr} [W]	86	315	172	118	733
m_{prop} [kg]	6.5	1.0	6.6	25.1	1.4
m_{ppu} [kg]	0.34	3.10	0.67	0.46	2.90
Inner Collector					
$P_{thruster}$ [W]	29	106	58	39	247
m_{prop} [kg]	2.3	0.3	2.3	8.7	0.5
m_{ppu} [kg]	0.12	1.00	0.23	0.15	0.97
Combiner					
$P_{thruster}$ [W]	~1	3	1	1	7
m_{prop} [kg]	0.3	~0	0.3	1.1	0.1
m_{ps} [kg]	35	62	47	36	122
m_{ppu} [kg]	~0	0.03	0.01	~0.01	0.03
P_{min}/P_{max} [W]	1610/1841	1610/2457	1610/2072	1610/1926	1610/3585
Total m_i [kg]	3250	3197	3263	3303	3331

Table 6: Calculated parameters for a tethered interferometer using different plasma propulsion systems. (For outer collectors: $m_{pay} = 593$[kg]; $\Delta V = 148$[m/s]. For inner collectors: $m_{pay} = 603$[kg]; $\Delta V = 52$[m/s]. For combiner: $m_{pay} = 625$[kg]; $\Delta V = 6$[m/s].)

Again, the advantage of decreased spacecraft/plume contamination exists for this structurally connected configuration. However, since the tether is not a rigid support, in order to perform the spin-up/spin-down maneuvers, thrusters must be located on all five components of the system to maintain their relative positions.

5.2 Results

For the tethered interferometer, the power supply is again located on the combiner module with the thruster power processing units co-located with the thrusters. There is now a ΔV associated with each component in the system as opposed to the monolith where there was only one for the whole system. All cases have a least one Li-ion battery, with the APPT possessing two, FEEP with three and the GF-PPT having a bank of eight.

5.3 Discussion

Even though each component is not rigidly attached to the others, there are sizable ΔV gains, again because the tether constrains the flight path of the spacecraft thus relieving the thrust requirement. The overall mass of the system is less than the monolith configuration. (Note this is mainly because in the monolithic architecture the trusses are taken to contribute 988 kg total to the spacecraft mass. This is the major mass difference between the tethered and monolith architectures.) The required peak power is slightly higher than that for the monolith because there are more thrusters firing at the same time in the tether case. In comparison to the free flyer, this configuration yields gains in power and propellant mass similar to the monolith configuration.

6 Conclusions

An overall comparison is made in Table 7 and Figure 5 between all the thruster/architecture combinations discussed in this paper. There is a breakdown of the major issues for each architecture in Figure 6. Finally, a matrix of the advantages and disadvantages of the various propulsion options, in this context, follows in Figure 7.

This study leads to the following conclusions.

- For the assumptions made, the initial masses of each architecture fall within the range of 3200 to 4200 kg.
- In general, the tether is the lowest in initial mass followed by the free flyer and then the monolith.
- These mN-thrust level propulsion tasks can be conducted in principle by any of these five types of thrusters. Specifically, the initial masses corresponding to any of these propulsion systems are all within 12% of each other for a given architecture.
- Furthermore, they all offer considerable advantages over any chemical propulsion option. (For example, when compared to a chemical thruster (I_{sp} = 350 s), a Hall thruster for the circular free flyer requires one-sixth the propellant mass with a minimal power supply penalty incurred).

	Hall	FEEP	APPT	AZPPT	GF-PPT
Free Flyer (circle)	3495	3391	3499	3716	3454
Free Flyer (square)	3495	3470	3509	3699	3866
Monolith	4063	4065	4077	4103	4145
Tether	3250	3197	3263	3303	3331

Table 7: A matrix showing total initial mass (m_i) in [kg] for each architecture and thruster combination.

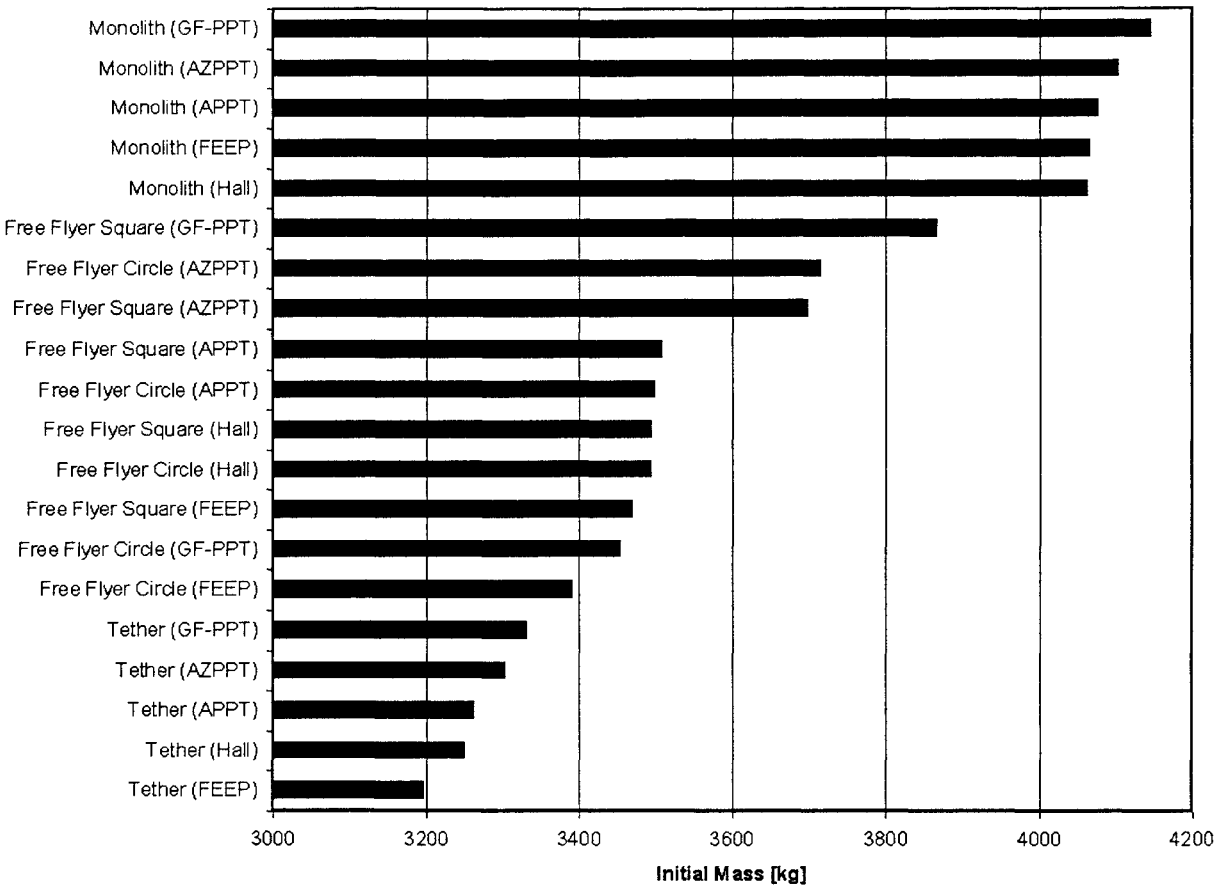

Figure 5: Stackup of the initial masses (m_i) for each architecture and thruster combination.

Since we found the *performance* of various plasma propulsion systems not to be an important differentiating index within a given architecture, measures of (a) the technology readiness and (b) the potential for spacecraft contamination by the exhaust plume products are more important parameters when choosing a thruster. As far a measure of readiness is concerned, the Hall thruster generally leads in technology readiness (as long as operation is maintained above 500 W), followed by the ablative PPT options, then FEEP and finally the GF-PPT. Having said this, it must be noted that the Hall thruster is never called upon in this study to operate above 500 W, so the development of a low power Hall thruster becomes a technology readiness issue. Also μN-level thrusters, which will be needed for formation keeping and attitude control in the free flyer but were not considered in the present study, remain to be life-tested in space. For the spacecraft contamination issue, cesium from FEEP presents the highest potential for spacecraft contamination, followed by Teflon from ablative PPTs and then by the Hall thruster and GF-PPT, both of which can operate with inert gases.

7 Acknowledgments

We acknowledge Joseph Troutman of Systems Design Concepts, Inc. and Andrew Horchler for their contributions to this paper.

This work was performed for the Jet Propulsion Laboratory, California Institute of Technology, sponsored by the National Aeronautics and Space Administration.

	Launch Mass/Configuration	Propulsion
Free Flyer	Medium overall mass. Attitude control using wheels/thrusters. More propellant for positioning control. Five separate solar arrays needed. Different thrusters required for μN and mN thrusting.	Thrusters used to position and constrain satellites in the cluster. Repointing of array neglected. Plume contamination of optics a large issue.
Monolith	Largest overall mass. Attitude control using wheels/thrusters. Potentially heavy truss deployment mechanism. Shared subsystems through truss conduits. One solar array needed.	Repointing of array the largest propellant drain. Structure constrains motion. Plume contamination of optics not a large problem.
Tether	Smallest launch mass. Possible elimination of some reaction wheels by use of multiple tethers between S/C. Less power needed in attitude and positioning control. Less on-board propellant due to reduced propulsion requirements. Shared subsystems by running conduits along the tethers between S/C.	Repointing of array the largest propellant drain. Tethers constrain motion. Less thrusting needed for attitude control by use of multiple tethers between S/C.
	Modeling/Simulation	**Stability/Control**
Free Flyer	Multiple degree of freedom (DOF) system; considerable modeling uncertainties.	Stability and positioning should be controlled using advanced control algorithms. Multi-sensor system. Data fusion and distributed estimation algorithms should be synthesized.
Monolith	Modeling via 6-DOF simulations relatively straightforward.	Stability, control and estimation quite straightforward.
Tether	Suitable approximations must be made. Single continuous system more difficult to simulate than individual spacecraft. Higher numerical precision required.	Control less straightforward. Stability may require minimal rotation velocity. Damping of tether motion is required.
	Manufacturing Costs	**Performance Limits**
Free Flyer	Considerable	Precision of sensors, robustness of optical array.
Monolith	Moderate	Structural constraints. Robustness of optical arrays. Constrained baseline.
Tether	Moderate	Critical tension imposes maximum rotational velocity. Elastic and thermal properties of tether. Risk of tether destruction by micrometeorites and orbital debris. Somewhat constrained baseline.

Most Desirable or Simplest	
Moderately Desirable or Difficult	
Least Desirable or Most Difficult	

Figure 6: A table showing the advantages/disadvantages of each architecture.

	Pros	Cons
Hall	• Moderate I_{sp} and High T/P ratio give rise to reasonable propellant mass and power requirements. • Space proven technology. • Low plume contamination risk.	• Higher fixed mass and complexity due to tankage & valves. • Presently limited to operation above 500 W. Low power Hall thruster not yet ready.
FEEP	• High I_{sp} leads to low propellant mass. • Low overall system mass.	• Low T/P gives rise to high power requirements. • High α leads to heavy PPU. • Thruster lifetime unknown. • Untested in space. • Contamination by cesium plume. • More thrust required in some cases than current FEEP systems can produce.
APPT	• Moderate I_{sp} and T/P ratio give rise to reasonable propellant mass and power requirements. • Space proven technology. • System simplicity and reliability.	• Higher fixed mass due to capacitor. • Contamination by Teflon plume.
AZPPT	• High T/P ratio gives rise to reasonable power requirements. • Space proven technology. • System simplicity and reliability.	• Low I_{sp} leads to high propellant mass. • Higher fixed mass due to capacitor. • Contamination by Teflon plume.
GFPPT	• High I_{sp} leads to low propellant mass. • Low plume contamination risk.	• Low T/P ratio gives rise to high power requirements. • Higher fixed mass and complexity due to tankage and capacitor.

Figure 7: A table showing the different advantages/disadvantages of each propulsion system.

References

[1] TPF Science Working Group. *Terrestrial Planet Finder*. NASA Jet Propulsion Laboratory, 1999.

[2] R.L. Stephenson. "Comparative system trades between structurally connected and separated spacecraft interferometers of the Terrestrial Planet Finder mission". Master's thesis, MIT, 1998.

[3] R.G. Jahn and E.Y. Choueiri. "Electric propulsion". *An Article for the Academic Press Encyclopedia of Physical Science and Technology (pre-print)*, April 2000.

[4] J.M. Troutman. *Solar cell sizing spreadsheet*. System Design Concepts, Inc., Lawrenceville, NJ.

[5] M. Martinez-Sanchez and J.E. Pollard. "Spacecraft electric propulsion - an overview". *Journal of Propulsion and Power*, 14(5):688–699, Sept.-Oct. 1998.

[6] S. Marcuccio, A. Genovese, and M. Andrenucci. "Experimental performance of field emission microthrusters". *Journal of Propulsion and Power*, 14(5):774–781, Sept.-Oct. 1998.

[7] P.J. Turchi and R.L. Burton. "Pulsed plasma thruster". *Journal of Propulsion and Power*, 14(5):716–735, Sept.-Oct. 1998.

[8] T.E. Markusic, K.A. Polzin, J.Z. Levine, C.A. McLeavey, and E.Y. Choueiri. "Ablative Z-pinch pulsed plasma thruster". In 36th *Joint Propulsion Conference*, Huntsville, AL, July 16-19, 2000. AIAA 2000-3257.

[9] J.K. Ziemer and E.Y. Choueiri. "Scaling laws for electromagnetic pulsed plasma thrusters". *Plasma Sources Science and Technology*, 10(3):395–405, Aug. 2001.

[10] V. Khayms and M. Martinez-Sanchez. "Design of a miniaturized Hall thruster for microsatellites". In 32th *Joint Propulsion Conference*, Lake Buena Vista, FL, July 1-3, 1996. AIAA 96-3291.

[11] Y. Raitses, N.J. Fisch, K.M. Ertmer, and C.A. Burlingame. "A study of cylindrical Hall thruster for low power space applications". In 36th *Joint Propulsion Conference*, Huntsville, AL, July 16-19, 2000. AIAA 2000-3421.